Appendix S1 – Supporting Information
Birds and bats differ in pest control pathways in fruit orchards: intraguild and direct predation

Details on field and laboratory procedures and complementary results

Details on field procedures in apple and blueberry orchards

Bird sampling

We characterized bird assemblages in three apple orchards and three blueberry orchards (Fig. S1.2). In apple orchards, we conducted 30-min point counts at one sampling location in each orchard, 25 m away from orchard edges, twice a month from August 2019 to July 2020. If meteorological conditions permitted, the three orchards were surveyed in succession on the same morning. To prevent temporal biases, the order of visits to the orchards was randomly selected for each set of surveys (i.e. every fortnight). Surveys were conducted by a single observer, beginning no earlier than 0730 hr and concluding no later than 1230 hr in the afternoon. The observer identified species and counted all individuals heard or seen in a 50-m radius from the sampling location (Ralph et al. 1995). Previous training, and the use of a plot map based on an aerial photograph helped to accurately locate bird observations within the apple plantation and the adjacent hedgerows despite the presence of woody cover. Bird individual movements and bird calls allowed species to be distinguished even under conditions of low visibility due to dense foliage, within the 50-m radius distance. When possible, we discarded repeated observations attributable to the same individual that had remained in the plot during a given observation period (e.g. individuals that appear intermittently at the same perching site within short time periods). Birds observed to be flying at an altitude exceeding 50 m without making any stops at the sampling location were not considered. In blueberry orchards, we conducted the sampling twice a month from May to September 2022. The sampling protocol was the same as for the apple crop, with the exception that we conducted 15-min point counts at two sampling locations: one close to the edge and one in the centre of the crop. We grouped the data from the three orchards of each crop and estimated the relative abundances of birds as the cumulative number of individuals recorded across all orchards and surveys over a year. We assume that this bird abundance metric might, despite our efforts, include some repeated counting of individual birds, and thus it must be considered as an estimate of bird activity across sites in functional terms, rather than a measure of local bird population sizes.

In the same orchards of surveys, we captured birds with mist nets and collected fresh faecal samples, following a common methodology in mist-netting studies (Parrish et al. 1994; Karp et al. 2013). We conducted mist-netting in apple orchards from August 2019 to July 2020, and in blueberry orchards from May to October 2022 and 2023. For each session, we placed two 9-18 m long and 2.5-3 m high mist nets with a mesh size of 16x16 mm (total capture area of 178.5 m²) inside the apple plantation and three nets at plantation borders (as bird activity is usually higher there), 2 m from woody hedgerows. Nets were set just before dawn and removed around noon, remaining open for five consecutive hours and checked for bird captures every 45–60 min. Captured birds were kept up to 40 min inside clean ringing cloth bags to collect faeces. Cloth bags were sterilized after every ringing session by machine washing them with bleach. All captured birds were marked with a uniquely numbered aluminium ring. Before release, each bird was weighed (digital balance; 0.1 g) and measured for Kipp's distance (distance between the tip of the first primary feather and the tip of the longest primary feather in the folded wing; flattened chord; 0.5 mm), tarsus length, and gape width (digital calliper; 0.1 mm). We collected faecal samples from the cloth bags using sterile swabs and stored them in the field at 4 °C until final storage at -20 °C in the laboratory.

Bat sampling

We recorded bat activity in 20 apple orchards and three blueberry orchards, including the orchards used for bird sampling (Fig. S1.2). From spring to autumn 2022, we conducted four sampling sessions (mid-May, mid-July, early September, and early October) using acoustic detectors (AudioMoth, Open Acoustic Devices; Hill et al., 2019) that recorded bats from 30 min before sunset until 30 min after sunrise. In blueberry

orchards, detectors were active during two consecutive nights. To improve detectability and sound quality, we mounted detectors on 3.5-m poles, above crop canopies. Sampling was conducted during good weather conditions (no precipitation; minimum temperature at night >12ºC; wind speed <3 m/s). All WAV sound files were screened using Kaleidoscope (v. 5.4.8, Wildlife Acoustics) and SonoBat (v. 4.2.2, International SonoBat, Arcata, CA, USA) software, in that order, to select those containing bat calls (positive files). All positive files were then screened and assigned to bats at the finest possible taxonomic level. To ensure consistency of classification, identifications were made by a single expert in the local bat fauna. This expert could refine the identification by considering the probability of each species occurring in the study area. We used the total time of bat calls recorded for each orchard and night as an indicator of the relative abundance of bat species by crop type (see Miñarro and García, 2025 for more details and for a description of the bat assemblage).

We collected bat faecal samples across the study area, in 17 roosts located within a maximum distance of 1 km from apple orchards (Fig. S1.1). Roosts were in human structures and nest boxes within 1 km of orchards. The roost network included abandoned houses, stables, sheds, churches, and bat artificial roosts installed within the study orchards. We visited roosts approximately every two weeks from spring 2022 to autumn 2023. To collect faecal samples, we placed collecting sheets under the bat perches, replacing them after every sampling. Likewise, we cleaned the bottoms of the nest boxes after each collection. During each visit, we collected up to 10 individual faecal samples per roost site using sterile forceps. Each sample consisted of 1 to 14 pellets (mean: 3.1, SE = 0.1) and was stored at -20 ºC until DNA extraction. We identified the bat species using a DNA barcoding approach through Sanger sequencing.

Spider sampling

We sampled spiders in 10 apple orchards in June 2016 (Fig. S1.2). In each orchard, we randomly selected 24 apple trees and sampled three branches per tree (approximately 1-m long) using the beating method. Three taps were given per branch, and all falling arthropods were collected in a plastic tray (80 x 50 x 8 cm) held below. To reduce the risk of contamination, spiders were transferred directly to individual tubes containing 95% ethanol. In blueberry, we collected spiders in three orchards on four separate occasions from May to September of 2022 (Fig. S1.2). Spiders were collected directly from blueberry plants with entomological forceps and placed individually into 2-ml plastic microcentrifuge tubes. We collected approximately 30 spiders per orchard each time. Collected individuals were identified to the most resolved taxonomic level and stored at -20 °C until DNA extraction. The species relative abundance was calculated by pooling all spiders collected across the 10 orchards of each crop.

Details on molecular and bioinformatic procedures for data obtained in apple and blueberry orchards

We detailed here the specific protocol employed to analyse each set of samples.

Bird samples from apple orchards

We analysed 546 samples from 26 different bird species captured in apple orchards. We extracted DNA from the samples using a silica solid-phase protocol, modifying the methods of Longmire et al., (1997) and Rohland and Hofreiter (2007). Samples were incubated overnight with Longmire (BE) and MixPK buffers at 37°C, then centrifuged them for 2 min at 9,600 g, and transferred the supernatant of each sample to clean tubes. We carried out the process of DNA adsorption using 80 µL silica per sample and a high guanidine thiocyanate salt concentration buffer. We washed DNA adsorbed onto the silica with wash buffer. Low pH conditions were maintained by the addition of 90 µl of

sodium acetate 3M. DNA adsorbed to the silica was profusely washed with Wash Buffer (ethanol 50%, 0.01 M Tris-HC 8 ph 8, 0.001 M EDTA ph 8, and 0.125 M NaCl). Finally, we loaded supernatant onto empty spin columns, we added 60 µL TE buffer, and centrifuged samples at 16,000 g for 1 min.

In the polymerase chain reaction (PCR) amplification, we used the primer pairs LepF1 (5′ ATT CAA CCA ATC ATA AAG ATA TTG G 3′) (Hebert et al., 2004)/ZBJ-ArtR2c-deg (5′ WAC TAA TCA ATT WCC AAA HCC HCC 3′) (Shutt et al., 2020) to amplify in 2 reactions a 178-base pair (bp) region of the mitochondrial cytochrome c oxidase (COI). Illumina sequencing primers were attached to these primers at their 5′ ends. PCRs were performed in a final volume of 25 µl, containing 2.5 µl of template DNA, 0.5 µM of the primers, 12.5 µl of Supreme NZYTaq 2x Green Master Mix (NZYTech), and ultrapure water up to 25 µl. The conditions were the following: an initial denaturation step at 95 ºC for 5 min, then 35 cycles of denaturing at 95 ºC for 30 s, annealing at 49 ºC for 45 s, and extension at 72 ºC for 45 s, followed by a final extension step at 72 ºC for 7 min. Individual barcodes were attached in a second PCR round with identical conditions except for the number of cycles, only 5, and the annealing at 60 ºC. A negative control that contained no DNA (BPCR) was included in every PCR round to check for contamination during library preparation. We verified library size in 2% agarose gels and purified libraries using the Mag-Bind RXNPure Plus magnetic beads (Omega Biotek). Then, we quantified libraries using Qubit dsDNA HSAssay (Thermo Fisher Scientific) and pooled them equimolarly. Finally, we purified and sequenced the pooled library in a NovaSeqPE250 run (Illumina). We used FastQC software (Andrews, 2010) to check the quality of demultiplex raw files and detect the Illumina adaptors, which were trimmed using CUTADAPT (Martin, 2011), and the paired reads were merged with FLASH2 (Magoč and Salzberg, 2011). Filtering based on the length of the fragment, the number of mismatches in the primers (up to 2), and the quality (Phred quality score ≥20) was applied. Next, we dereplicated filtered sequences (-derep fulllength) using the VSEARCH bioinformatic tool (Rognes et al., 2016). We carried out de novo chimera detection using the UCHIME algorithm (Edgar et al., 2011) implemented in VSEARCH. Finally, sequences were clustered at a similarity threshold of 98 % (-cluster fast, -centroidsoption) following Shutt et al. (2020).

We performed the taxonomic identification using the script classify-consensus-VSEARCH implemented in Qiime2 (Bokulich et al., 2018) and the VSEARCH algorithm (Rognes et al., 2016) with a sequence similarity threshold of 90%. We used the Robeson et al., (2021) database for the taxonomic identification of the sequences. Singletons (i.e., OTUs containing only one-member sequence in the whole data set), OTUs occurring at a frequency < 0.1 % in each sample, and unassigned OTUs were removed. In addition, from animal sequences only taxa within the phyla Arthropoda were selected and as a result, six samples ended up without sequences and were dropped from the subsequent. We checked taxonomic identification on a case-by-case basis and modified when necessary. This is because in some cases, automatic identification cannot differentiate between closely related species due to the small fragment of COI used, and may even sometimes identify species that are not present in the study area (likely because the specific sequence is not available in public archives). We also removed those OTUs occurring at a frequency of <0.1% in each sample to avoid cases of accidental and secondary consumption (Deagle et al., 2019).

Bird samples from blueberry orchards and bat samples

We analysed 282 samples from 11 bird species and 375 samples from five different bat species. We extracted DNA from the samples using a silica solid-phase protocol, modifying the methods of Longmire et al., (1997) and Rohland and Hofreiter (2007). Samples were incubated overnight with Longmire (BE) and MixPK buffers at 37°C, then centrifuged them for 2 min at 9,600 g, and transferred the supernatant of each sample

to clean tubes. We carried out the process of DNA adsorption using 80 µL silica per sample and a high guanidine thiocyanate salt concentration buffer. We washed DNA adsorbed onto the silica with wash buffer. Low pH conditions were maintained by the addition of 90 µl of sodium acetate 3M. DNA adsorbed to the silica was profusely washed with Wash Buffer (ethanol 50%, 0.01 M Tris-HC 8 ph 8, 0.001 M EDTA ph 8, and 0.125 M NaCl). Finally, we loaded supernatant onto empty spin columns, we added 60 µL TE buffer, and centrifuged samples at 16,000 g for 1 min.

Bat species identification was confirmed using a DNA barcoding approach through Sanger sequencing. Because we expected to get low-quality and low-quantity DNA from faecal samples, we used DNA mini-barcode primers specifically designed for Chiropteran species. We amplified a region of the Cytochrome Oxidase subunit I (COI) gene using the primers SFF_145f (5' GTHACHGCYCAYGCHTTYGTAATAAT 3') and SFF_351r (5' CTCCWGCRTGDGCWAGRTTTCC 3') for all faecal samples (Walker et al., 2016). Polymerase chain reactions (PCR) were set up in a total volume of 10 µl, including 5 µl of 2x QIAGEN Multiplex PCR Master Mix, 0.5 µl (10 mM) of each primer and 1.5 µl of genomic DNA. PCRs were performed under the following conditions: initial hot-start denaturation at 95 °C for 15 min; followed by 40 cycles of denaturation at 95 °C for 60 s, annealing at 56 °C for 30 s, and extension at 72 °C for 30 s; concluding with a final extension at 60 °C for 30 min. All PCRs included two negative controls. PCR products were visualised on 1.5% agarose gels stained with GelRed®. Sequencing of the PCR products was performed using the Perkin Elmer BigDye terminator (v. 3.1), with primer SFF_145f. Sequences were aligned manually using BioEdit version 7.01 (Hall, 1999) and Chromas Lite (https://technelysium.com.au/wp/chromas/). We used both NCBI's BLAST and BOLD Identification System tool to identify the bat species. A few samples from roosts inhabited by more than one species could not be confidently assigned to a single species, presumably because the pellets originated from different bat species, and were therefore excluded from the diet analysis.

To determine the prey composition of bird samples from blueberry orchards and bat samples, we followed a similar metabarcoding approach that with birds. In the PCR amplification, the primer pairs LepF1 (5′ ATT CAA CCA ATC ATA AAG ATA TTG G 3′) (Hebert et al., 2004) / ZBJ-ArtR2c-deg (5′ WAC TAA TCA ATT WCC AAA HCC HCC 3′) (Shutt et al., 2020) weas used to amplify in two reactions a 225 bp region of the mitochondrial COI. These primers also included the Illumina sequencing primer sequences attached to their 5' ends. PCRs were carried out in a final volume of 12.5 µL, containing 1.25 µL of template DNA, 0.5 µM of the primers, 6.25 µL of Supreme NZYTaq 2x Green Master Mix (NZYTech), and ultrapure water up to 12.5 µL. The reaction mixture was incubated as follows: an initial denaturation step at 95 ºC for 5 min, followed by 35 cycles of 95 ºC for 30 s, 49 ºC for 1min, 72 ºC for 45 s, and a final extension step at 72 ºC for 7 min. Individual barcodes were attached in a second PCR round with identical conditions except for the number of cycles, only 5, and the annealing at 60 ºC. A negative control that contained no DNA (BPCR) was included in every PCR round to check for contamination during library preparation. The library size was verified by running the libraries on 3 % agarose gels stained with GreenSafe (NZYTech) and imaging them under UV light. Then, the libraries were purified using the Mag-Bind RXNPure Plus magnetic beads (Omega Bio-tek), following the instructions provided by the manufacturer. Finished libraries were pooled in equimolar amounts according to the results of a Qubit dsDNA HS Assay (Thermo Fisher Scientic) quantification. The pool was sequenced in a fraction of a NovaSeq PE250 flow cell (Illumina) aiming for a total output of 18 gigabases. We used FastQC software (Andrews, 2010) to check the quality of demultiplex raw files and detect the Illumina adaptors, which were trimmed using CUTADAPT (Martin, 2011), and the paired reads were merged with FLASH2 (Magoč and Salzberg, 2011). Then, the amplicon reads were processed using the tool DADA2 (Callahan et al., 2016) implemented in QIIME 2 (Bolyen et al., 2019). Dereplication of the dataset was carried out, and dereplicated forward and reverse reads were used to

infer Amplicon Sequence Variants (ASVs) with the core sample inference algorithm (Callahan et al., 2016). Subsequently, corresponding R1 and R2 reads were merged into pairs with a minimum overlap of 12 identical base pairs. Finally, PCR and sequencing artefacts, such as chimaeras, were removed.

Taxonomic assignment of each ASV was conducted using a pre-trained classifier of the COInr reference database (Meglecz, 2022; version 2023-05-03 with additional polishing by AllGenetics). To compare the sequence of each ASV to the reference database, and compute the taxonomic assignment, the algorithm VSEARCH was employed (Rognes et al., 2016), which is implemented in QIIME 2 as the feature-classifier approach classify-consensus-vsearch (Bokulich et al., 2018). A minimum percent identity of 90% was set. Singletons (i.e. ASVs containing only one-member sequence in the whole data set) and unidentified sequences were removed. In addition, only taxa within the phylum Arthropoda were selected and as a result. We checked taxonomic identification on a case-by-case basis and modified it when necessary, and we also removed those OTUs occurring at a frequency of <0.1% in each sample to avoid cases of accidental and secondary consumption (Deagle et al., 2019).

Spider samples from apple orchards

We included 227 samples from 53 different spider species collected in apple orchards. DNA was extracted from dissected abdomens, for larger specimens, and whole abdomens for smaller specimens. In order to avoid contamination, we handled each sample separately using disposable gloves, sterile Petri dishes and blades in UV cabinets, while working surfaces were cleaned after each dissection with 70% ethanol. The spider tissue was placed in a sterile Eppendorf tube and we performed DNA extraction using the QIAamp DNA Micro Kit (Qiagen, www.qiagen.com), following the manufacturer's instructions.

We sequenced three sections, depending on predator taxon, within the Folmer region of COI (Folmer et al., 1994). In the PCR amplification, we used the primer pairs NoAranR (5´ TGTTCATCCDGTNCCWG 3´) (Hambäck et al., 2021) / LCO146 (5´ GGTCAACAAATCATAAAGATATTGG 3´) (Folmer et al., 1994) to amplified a 317 bp fragment, NoOpiF (5´ CCHGAYATAGCWTTYCCHCGAATA 3´) (Hambäck et al., 2021) / fwhR2n (5' GTRATWGCHCCDGCTARWACWGG 3') (Vamos et al., 2017) to amplified a 306 bp fragment, and NoSpi2 (5´ TTYCCHCGWATAAAYAAYATAAG 3´) (Lafage et al., 2020) / fwhR2n to amplified a 295 bp fragment. For post-process identification of individual spider guts, we used a dual tagging approach. In the PCR, an eight base pair-tag was included on the 5´-end of the primers (Binladen et al., 2007) and thereafter Illumina adaptors bearing unique indices were ligated to the phosphorylated amplicons. Sequencing was done in two batches using parallel high throughput sequencing on the Illumina MiSeq3 platform at SciLifeLab in Stockholm, one involving NoAranR and one involving NoOpiF and NoSpi2. Sequence data was processed using OBITOOLS 1.2.9 (Boyer et al., 2016) as described in Verschut et al., (2019). PE-sequences with a minimum combined quality score of 40 were assembled, trimmed from PCR primers and demultiplexed after filtering into individual samples according to their respective tagged primer and index combination using NGSFILTER. The reads were dereplicated with the "obiuniq" command and filtered the data for PCR errors with the "obiclean" command by keeping "head" sequences (sequences with no variants with a count >5% of their own count) and discarding singletons and erroneous sequences (sequences with a count <5% of their own count; Boyer et al., 2016).

ASVs were identified using a 97% similarity threshold in the Barcode of Life Database (www.boldsystems.org; Ratnasingham and Hebert, 2007), and pooled sequence counts to lowest taxon identity. Some sequences could not be sorted to species, due to low variability in target sequences. Contaminations (human, cow and bird DNA) and sequences identified as plant identities, fungal or bacterial were discarded. Sequences

belonging to the same genus as the consumer individual were also discarded. As a final cleaning step, a probabilistic approach was used to remove potential tag jumping errors through a combination of fixed and species-specific thresholds. We used a probabilistic approach to remove potential tag jumping errors through a combination of fixed and species-specific thresholds (see Hambäck et al., 2021 for mor details). We checked taxonomic identification on a case-by-case basis and modified it when necessary.

Spider samples from blueberry orchards

We extracted DNA from the whole abdomens of spiders using the DNeasy Blood & Tissue Kit (Qiagen, www.qiagen.com), following the manufacturer's instructions. Specifically, we followed the protocol designed for the purification of DNA from up to 50 mg of insects using disposable microtube pestles.

We sequenced three sections, depending on predator taxon, within the Folmer region of COI (Folmer et al., 1994). In the PCR amplification, we used the primer pairs NoAranR (5´ TGTTCATCCDGTNCCWG 3´) (Hambäck et al., 2021) / LCO146 (5´ GGTCAACAAATCATAAAGATATTGG 3´) (Folmer et al., 1994) to amplified a 317 bp fragment, NoSpi2 (5´ TTYCCHCGWATAAAYAAYATAAG 3´) (Lafage et al., 2020) / fwhR2n to amplified a 295 bp fragment, and the general primer pair LepF1 (5′ ATT CAA CCA ATC ATA AAG ATA TTG G 3′) (Hebert et al., 2004) / ZBJ-ArtR2c-deg (5′ WAC TAA TCA ATT WCC AAA HCC HCC 3′) (Shutt et al., 2020) to amplify a 225 bp fragment. These primers also included the Illumina sequencing primer sequences attached to their 5' ends. The exact parameters of the PCRs varied slightly between primer pairs. PCRs were carried out in a final volume of 12.5-25 µL, containing 1-3.18 µL of template DNA, 0.5-2 µM of the primers, 6.25-7.81 µL of Supreme NZYTaq 2x Green Master Mix (NZYTech), and ultrapure water up to 12.5 µL. The reaction mixture was incubated as follows: an initial denaturation step at 95ºC for 5 min, followed by 35 cycles of 95 ºC for 30 s, 49 ºC for 45 s, 72 ºC for 45 s, and a final extension step at 72 ºC for 7 min. Prior to library indexing, the PCR products were purified using the Mag-Bind RXNPure Plus magnetic beads (Omega Biotek), following the instructions provided by the manufacturer. Individual barcodes were attached in a second PCR round with identical conditions except for the number of cycles, only 5, and the annealing at 60 ºC. A negative control that contained no DNA (BPCR) was included in every PCR round to check for contamination during library preparation. The library size was verified by running the libraries on 2% agarose gels stained with GreenSafe (NZYTech) and imaging them under UV light. Finished libraries were pooled in equimolar amounts according to the results of a Qubit dsDNA HS Assay (Thermo Fisher Scientic) quantification. The pool was sequenced in a fraction of a NovaSeq PE250 flow cell (Illumina). We used FastQC software (Andrews, 2010) to check the quality of demultiplex raw files and detect the Illumina adaptors, which were trimmed using CUTADAPT (Martin, 2011), and we summarised the output using MultiQC (Ewels et al., 2016). Sequence data was processed using OBITOOLS 1.2.9 (Boyer et al., 2016) as described in Verschut et al., (2019). PE-sequences with a minimum combined quality score of 40 were assembled, trimmed from PCR primers and demultiplexed after filtering into individual samples according to their respective tagged primer and index combination using NGSFILTER. The reads were dereplicated with the “obiuniq” command and filtered the data for PCR errors with the “obiclean” command by keeping “head” sequences (sequences with no variants with a count >5% of their own count) and discarding singletons and erroneous sequences (sequences with a count <5% of their own count; Boyer et al., 2016).

ASVs were identified using a 97% similarity threshold in the Barcode of Life Database (www.boldsystems.org; Ratnasingham and Hebert, 2007), and pooled sequence counts to lowest taxon identity. Some sequences could not be sorted to species, due to low variability in target sequences. Contaminations (human, cow and bird DNA) and sequences identified as plant identities, fungal or bacterial were discarded. Sequences

belonging to the same genus as the consumer individual were also discarded. In addition, only taxa within the phylum Arthropoda were selected and as a result. We checked taxonomic identification on a case-by-case basis and modified it when necessary, and we also removed those OTUs occurring at a frequency of <0.1% in each sample to avoid cases of accidental and secondary consumption (Deagle et al., 2019).

References

Andrews, S. (2010). FastQC A Quality Control tool for High Throughput Sequence Data. https://www.bioinformatics.babraham.ac.uk/projects/fastqc/

Binladen, J., Gilbert, M. T. P., Bollback, J. P., Panitz, F., Bendixen, C., Nielsen, R., & Willerslev, E. (2007). The Use of Coded PCR Primers Enables High-Throughput Sequencing of Multiple Homolog Amplification Products by 454 Parallel Sequencing. PLOS ONE, 2(2), e197. https://doi.org/10.1371/journal.pone.0000197

Bokulich, N. A., Kaehler, B. D., Rideout, J. R., Dillon, M., Bolyen, E., Knight, R., Huttley, G. A., & Gregory Caporaso, J. (2018). Optimizing taxonomic classification of marker-gene amplicon sequences with QIIME 2's q2-feature-classifier plugin. Microbiome, 6(1), 90. https://doi.org/10.1186/s40168-018-0470-z

Bolyen, E., Rideout, J. R., Dillon, M. R., Bokulich, N. A., Abnet, C. C., Al-Ghalith, G. A… & Caporaso, J. G. (2019). Reproducible, interactive, scalable and extensible microbiome data science using QIIME 2. Nature Biotechnology, 37(8), 852-857. https://doi.org/10.1038/s41587-019-0209-9

Boyer, F., Mercier, C., Bonin, A., Le Bras, Y., Taberlet, P., & Coissac, E. (2016). obitools: A unix-inspired software package for DNA metabarcoding. Molecular Ecology Resources, 16(1), 176-182. https://doi.org/10.1111/1755-0998.12428

Callahan, B. J., McMurdie, P. J., Rosen, M. J., Han, A. W., Johnson, A. J. A., & Holmes, S. P. (2016). DADA2: High-resolution sample inference from Illumina amplicon data. Nature Methods, 13(7), 581-583. https://doi.org/10.1038/nmeth.3869

Deagle, B. E., Thomas, A. C., McInnes, J. C., Clarke, L. J., Vesterinen, E. J., Clare, E. L., Kartzinel, T. R., & Eveson, J. P. (2019). Counting with DNA in metabarcoding studies: How should we convert sequence reads to dietary data? Molecular Ecology, 28(2), 391-406. https://doi.org/10.1111/mec.14734

Edgar, R. C., Haas, B. J., Clemente, J. C., Quince, C., & Knight, R. (2011). UCHIME improves sensitivity and speed of chimera detection. Bioinformatics, 27(16), 2194-2200. https://doi.org/10.1093/bioinformatics/btr381

Ewels, P., Magnusson, M., Lundin, S., & Käller, M. (2016). MultiQC: Summarize analysis results for multiple tools and samples in a single report. Bioinformatics, 32(19), 3047-3048. https://doi.org/10.1093/bioinformatics/btw354

Folmer, O., Black, M., Hoeh, W., Lutz, R., & Vrijenhoek, R. (1994). DNA primers for amplification of mitochondrial cytochrome c oxidase subunit I from diverse metazoan invertebrates. Molecular Marine Biology and Biotechnology, 3, 294–297.

Hall, T.A. (1999) BioEdit: A User-Friendly Biological Sequence Alignment Editor and Analysis Program for Windows 95/98/NT. Nucleic Acids Symposium Series, 41: 95-98.

Hambäck, P. A., Cirtwill, A. R., García, D., Grudzinska-Sterno, M., Miñarro, M., Tasin, M., Yang, X., & Samnegård, U. (2021). More intraguild prey than pest species in arachnid diets may compromise biological control in apple orchards. Basic and Applied Ecology, 57, 1-13. https://doi.org/10.1016/j.baae.2021.09.006

Hebert, P. D. N., Penton, E. H., Burns, J. M., Janzen, D. H., & Hallwachs, W. (2004). Ten species in one: DNA barcoding reveals cryptic species in the neotropical skipper butterfly Astraptes fulgerator. Proceedings of the National Academy of Sciences, 101(41), 14812-14817. https://doi.org/10.1073/pnas.0406166101

Hill, A. P., Prince, P., Snaddon, J. L., Doncaster, C. P., & Rogers, A. (2019). AudioMoth: A low-cost acoustic device for monitoring biodiversity and the environment. HardwareX, 6, e00073. https://doi.org/10.1016/j.ohx.2019.e00073

Karp, D. S., Mendenhall, C. D., Sandí, R. F., Chaumont, N., Ehrlich, P. R., Hadly, E. A., & Daily, G. C. (2013). Forest bolsters bird abundance, pest control and coffee yield. Ecology Letters, 16(11), 1339-1347. https://doi.org/10.1111/ele.12173

Lafage, D., Elbrecht, V., Cuff, J. P., Steinke, D., Hambäck, P. A., & Erlandsson, A. (2020). A new primer for metabarcoding of spider gut contents. Environmental DNA, 2(2), 234-243. https://doi.org/10.1002/edn3.62

Longmire, J. L., Maltbie, M., & Baker, R. J. (1997). Use of «Lysis Buffer» in DNA isolation and its implication for museum collections. Museum of Texas Tech University. https://www.biodiversitylibrary.org/item/242562

Magoč, T., & Salzberg, S. L. (2011). FLASH: Fast length adjustment of short reads to improve genome assemblies. Bioinformatics, 27(21), 2957-2963. https://doi.org/10.1093/bioinformatics/btr507

Martin, M. (2011). Cutadapt removes adapter sequences from high-throughput sequencing reads. EMBnet.Journal, 17(1), Article 1. https://doi.org/10.14806/ej.17.1.200

Meglécz, E. (2022). COInr and mkCOInr: Building and customizing a non-redundant barcoding reference database from BOLD and NCBI using a lightweight pipeline. https://doi.org/10.1101/2022.05.18.492423

Miñarro, M., & García, D. (2025). Landscape composition and orchard management effects on bat assemblages and bat foraging activity in apple crops. Ecosphere, (e70140). https://doi.org/10.1002/ecs2.70140

Parrish, J. D., Whitman, M. L., & Comings, S. B. (1994). A Facilitated Method for Collection of Fecal Samples from Mist-netted Birds.

Ralph, C. J., Droege, S., & Sauer, J. R. (1995). Managing and Monitoring Birds Using Point Counts: Standards and Applications1,3.

Ratnasingham, S, & Hebert, P. D. N. (2007). BOLD: The Barcode of Life Data System (www.barcodinglife.org). Molecular Ecology Notes, 7, 355–364. https://doi.org/10.1111/j.1471-8286.2007.01678.x

Robeson, M. S., O'Rourke, D. R., Kaehler, B. D., Ziemski, M., Dillon, M. R., Foster, J. T., & Bokulich, N. A. (2021). RESCRIPt: Reproducible sequence taxonomy reference database management. PLOS Computational Biology, 17(11), e1009581. https://doi.org/10.1371/journal.pcbi.1009581

Rognes, T., Flouri, T., Nichols, B., Quince, C., & Mahé, F. (2016). VSEARCH: A versatile open-source tool for metagenomics. PeerJ, 4, e2584. https://doi.org/10.7717/peerj.2584

Rohland, N., & Hofreiter, M. (2007). Ancient DNA extraction from bones and teeth. Nature Protocols, 2(7), 1756-1762. https://doi.org/10.1038/nprot.2007.247

Shutt, J. D., Nicholls, J. A., Trivedi, U. H., Burgess, M. D., Stone, G. N., Hadfield, J. D., & Phillimore, A. B. (2020). Gradients in richness and turnover of a forest passerine's diet prior to breeding: A mixed model approach applied to faecal metabarcoding data. Molecular Ecology, 29(6), 1199-1213. https://doi.org/10.1111/mec.15394

Vamos, E. E., Elbrecht, V., & Leese, F. (2017). Short COI markers for freshwater macroinvertebrate metabarcoding. Metabarcoding and Metagenomics, 1, e14625. https://doi.org/10.3897/mbmg.1.14625

Verschut, V., Strandmark, A., Esparza-Salas, R., & Hambäck, P. A. (2019). Seasonally varying marine influences on the coastal ecosystem detected through molecular gut analysis. *Molecular Ecology*, *28*(2), 307-317. https://doi.org/10.1111/mec.14830

Walker, F.M., Williamson, C.H.D., Sanchez, D.E., Sobek, C.J., & Chambers, C.L. (2016). Species From Feces: Order-Wide Identification of Chiroptera From Guano and Other Non-Invasive Genetic Samples. PLoS ONE 11(9): e0162342.

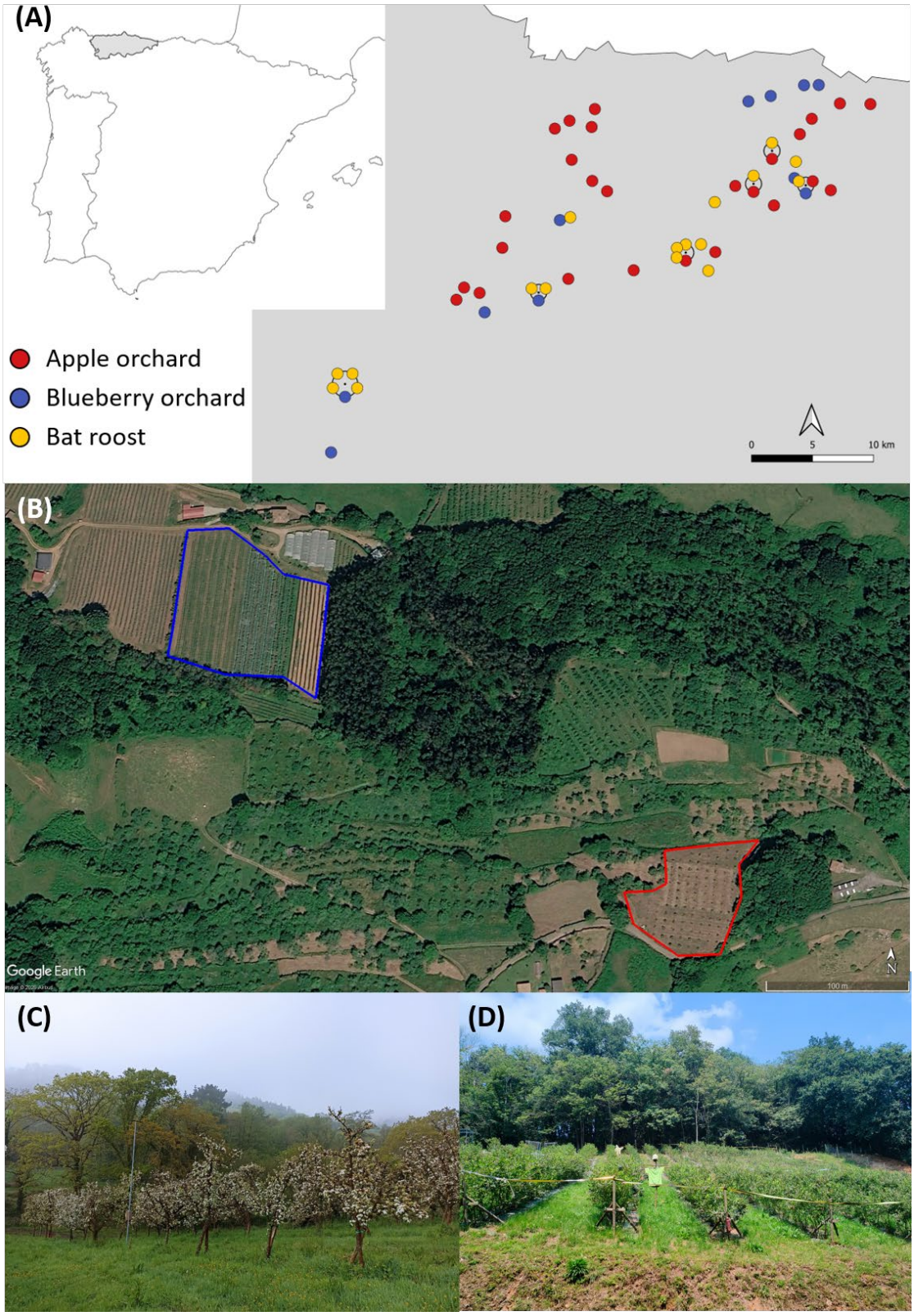

Fig. S1.1. (A) Schematic representation of study area, depicting the region of study (Asturias province in dark grey within the peninsular Spain), and the location of the apple orchards, blueberry orchards and bat roosts where data were collected. (B) Aerial view of an apple orchard (in red) and a blueberry orchard (in blue) in the study area. (C) Photograph of an apple orchard ©Marcos Miñarro. (D) Photograph of a blueberry orchard ©Manuel Soto.

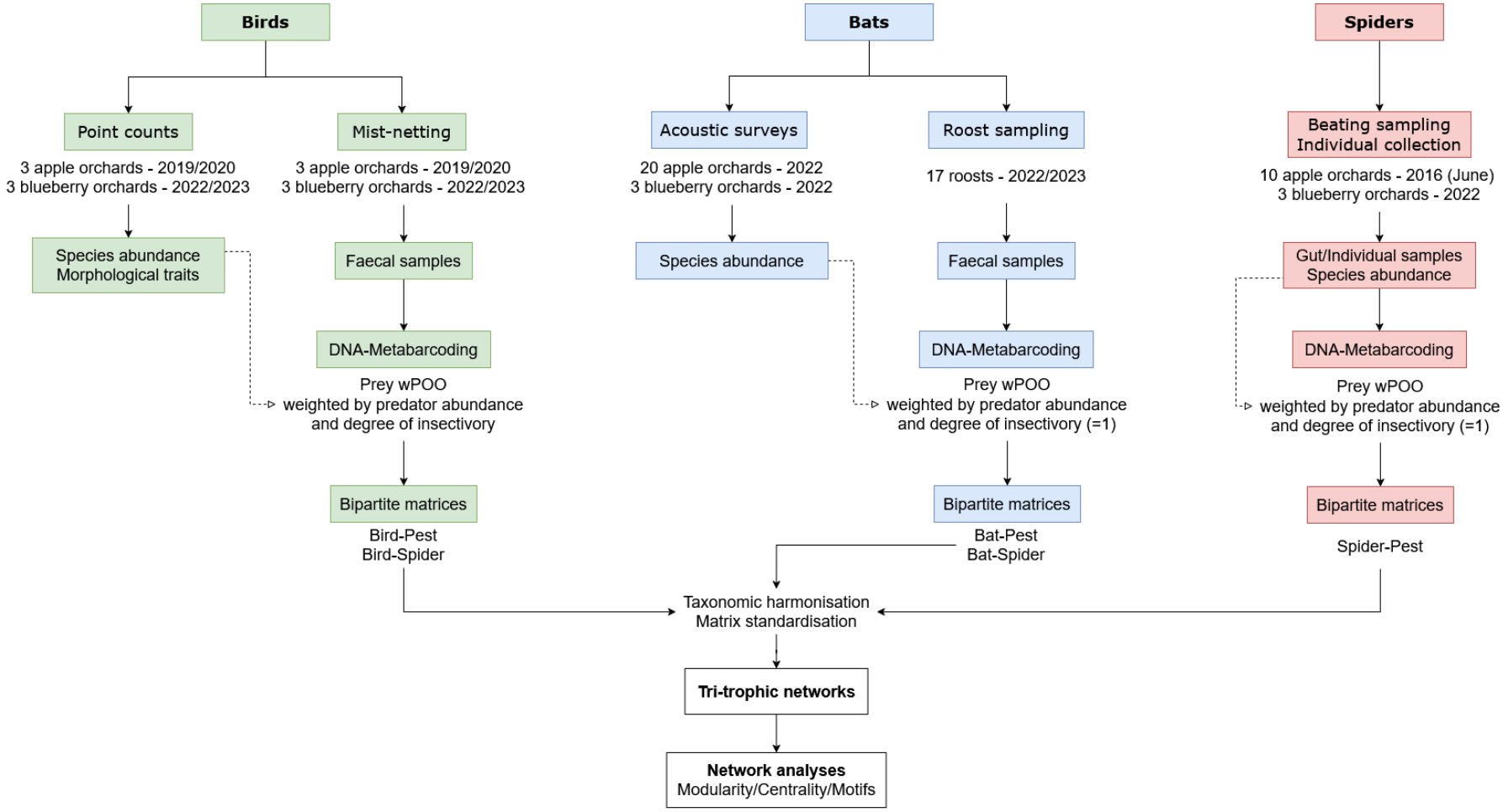

Fig. S1.2. Workflow of data integration and network construction. Bird, bat and spider datasets differed in sampling period, spatial coverage and data source. For each predator group, diet metabarcoding data were used to construct predator-prey interaction matrices. The resulting bipartite matrices were taxonomically harmonised and standardised before being merged into crop-specific tri-trophic networks. These networks were subsequently used to quantify modularity, species centrality and tri-trophic motifs.

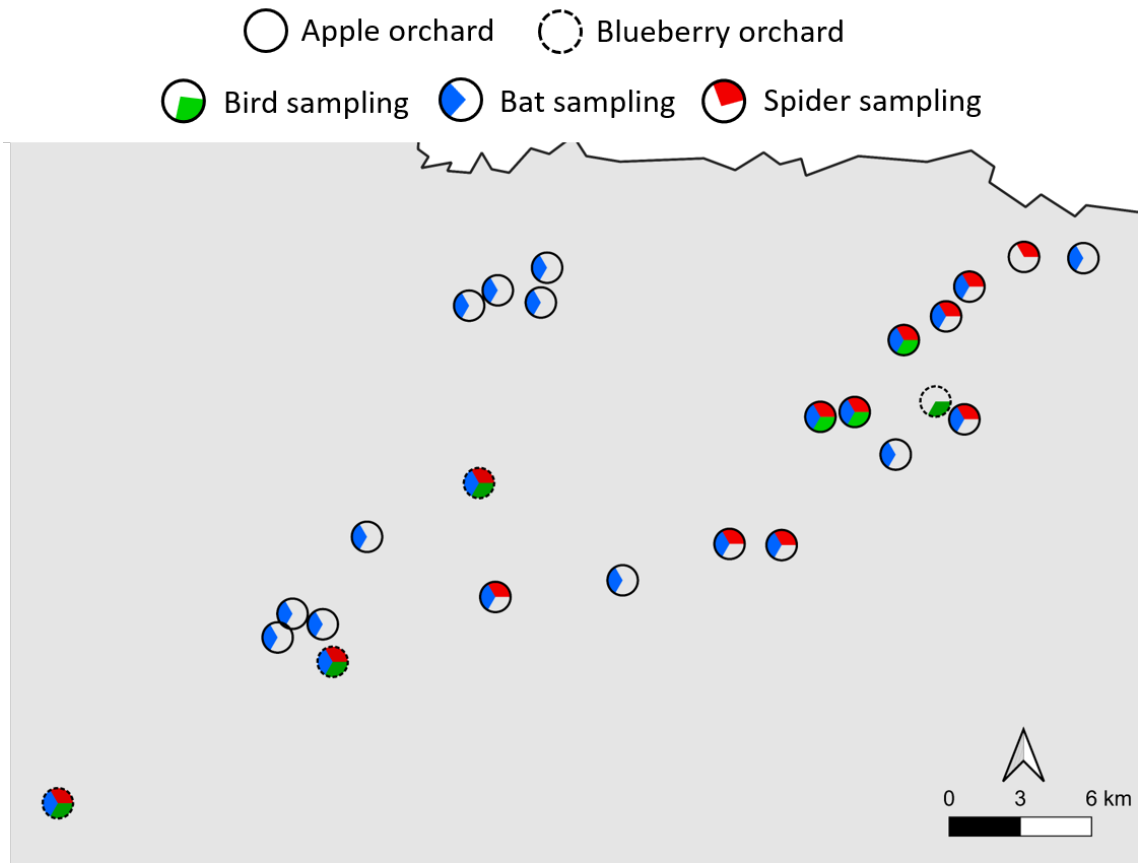

Fig. S1.3. Schematic representation of study area, depicting location of the apple and blueberry orchards where data were collected. Bird sampling consisted in bird censuses and mist-netting to collect fresh faecal samples. Bat sampling consisted in bat censuses with acoustic detectors (AudioMoth, Open Acoustic Devices). Spider sampling consisted in the collection of individual specimens.

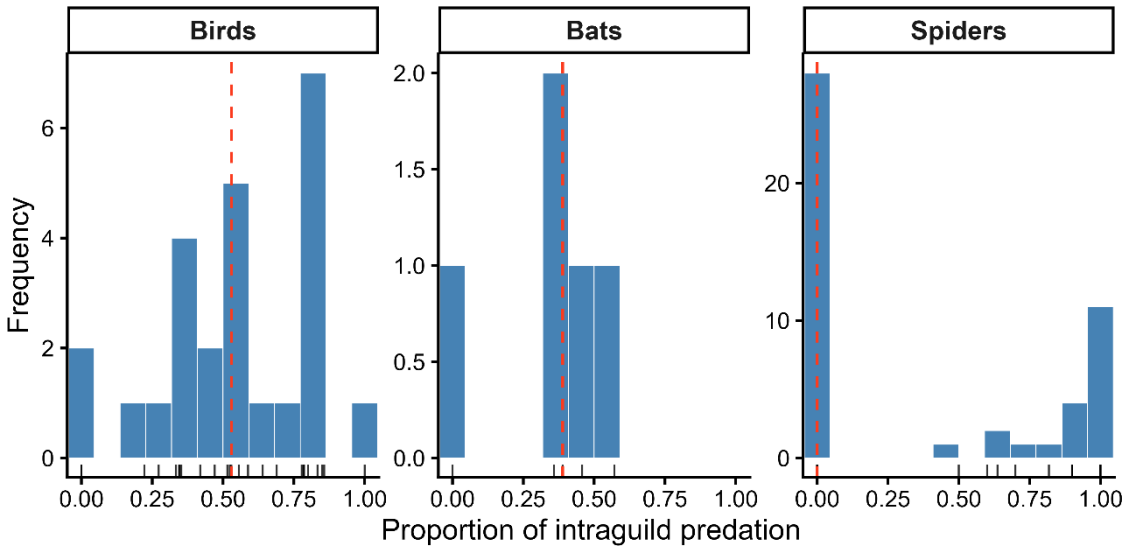

Fig. S1.4. Distribution of the proportion of intraguild predation (IGP) among bird, bat and spider taxa in the apple tri-trophic network. The histograms show species frequencies, with rug marks indicating individual observations. Red dashed lines represent median values.

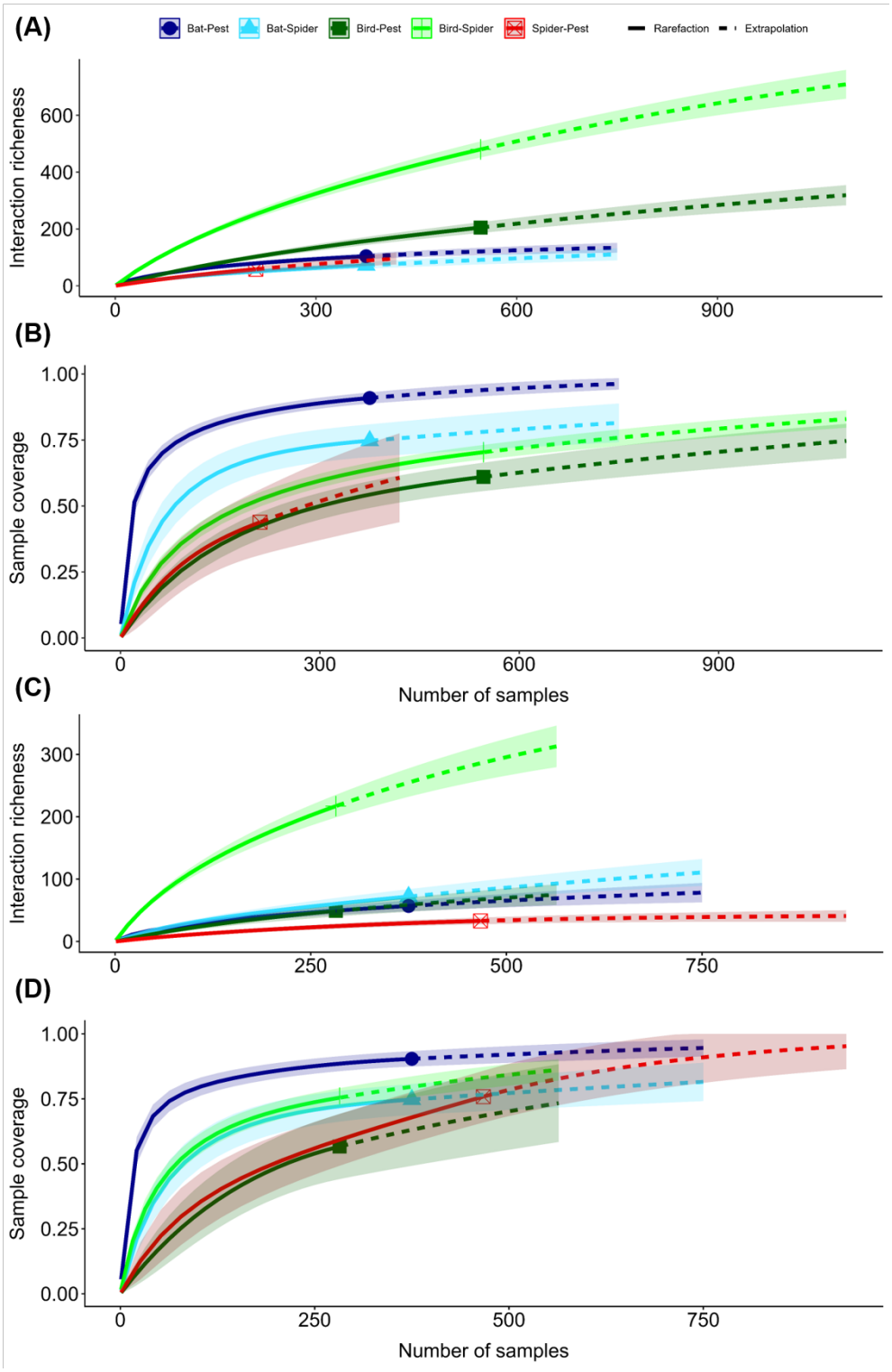

Fig. S1.5. Rarefaction curves of predator-prey interactions richness and sample coverage, per sampling effort unit (number of samples of predatory species analysed), for different interaction types. Symbols represent the observed values and the dashed line the extrapolated values expected with higher sampling effort. (A) and (B) show data from apple orchards; (C) and (D) show data from blueberry orchards.

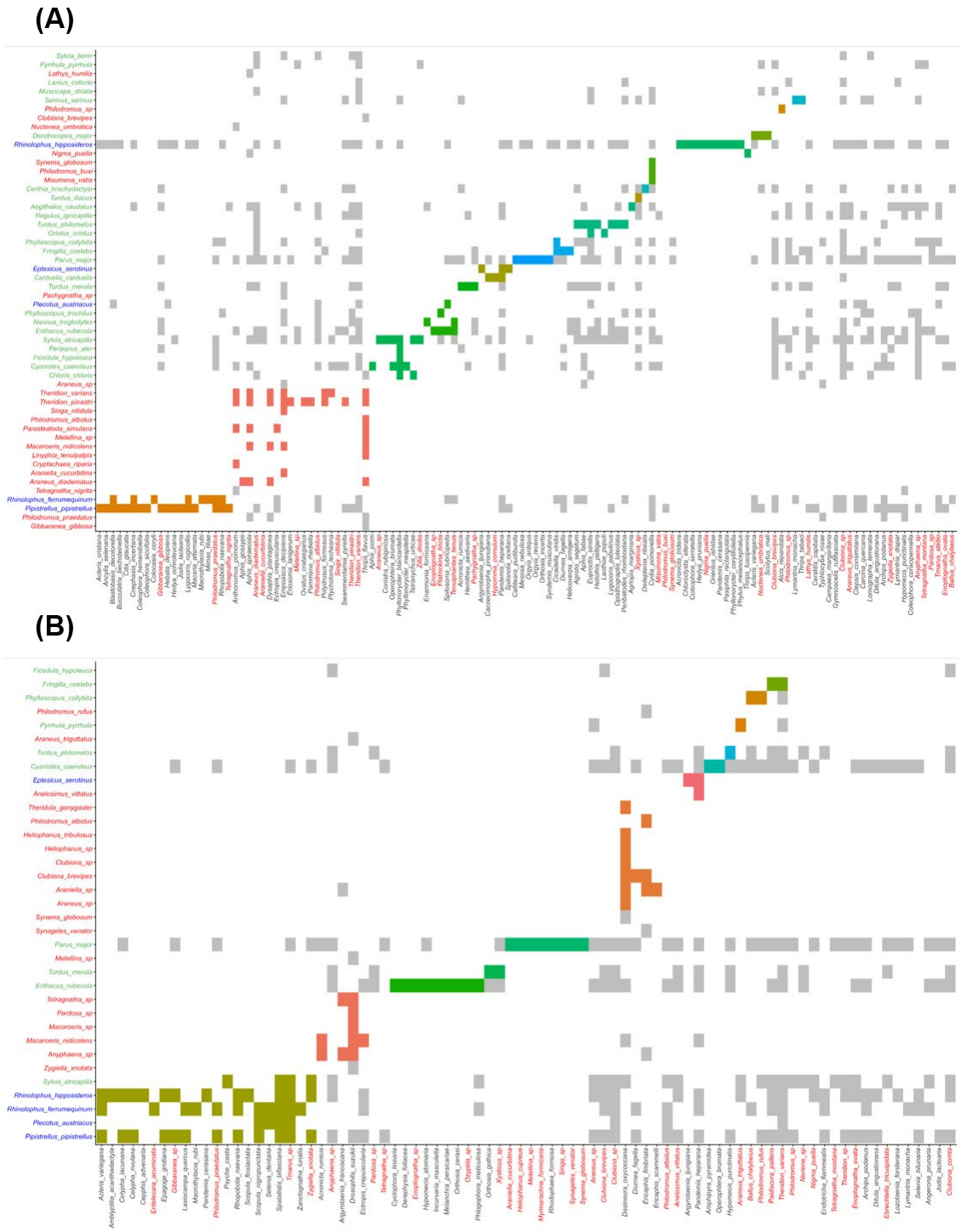

Fig. S1.6. Representation of the tri-trophic networks observed in (A) apple orchards and (B) blueberry orchards between vertebrates (birds in green and bats in blue), spiders (in red) and pests (in black). Actual interactions between species pairs are shown in coloured squares. Each colour represents interactions between species pairs belonging to the same module, and the grey squares represent those between species pairs belonging to different modules.

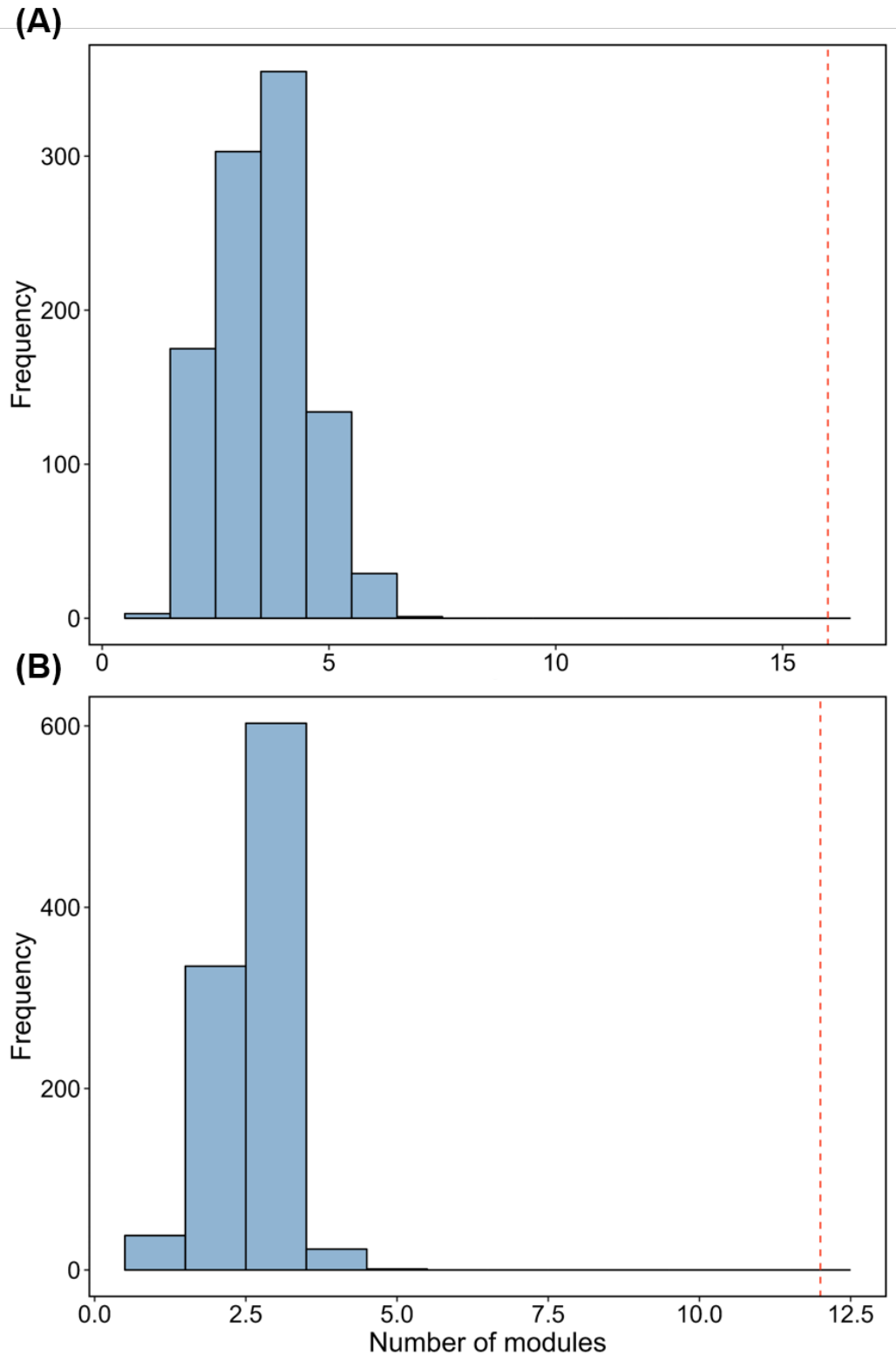

Fig. S1.7. Histograms with the frequency of the number of modules of 1,000 randomized networks originated by the Vaznull null-model in (A) apple orchards and (B) blueberry orchards. Red dashed line represents the number of modules in the observed tritrophic network.

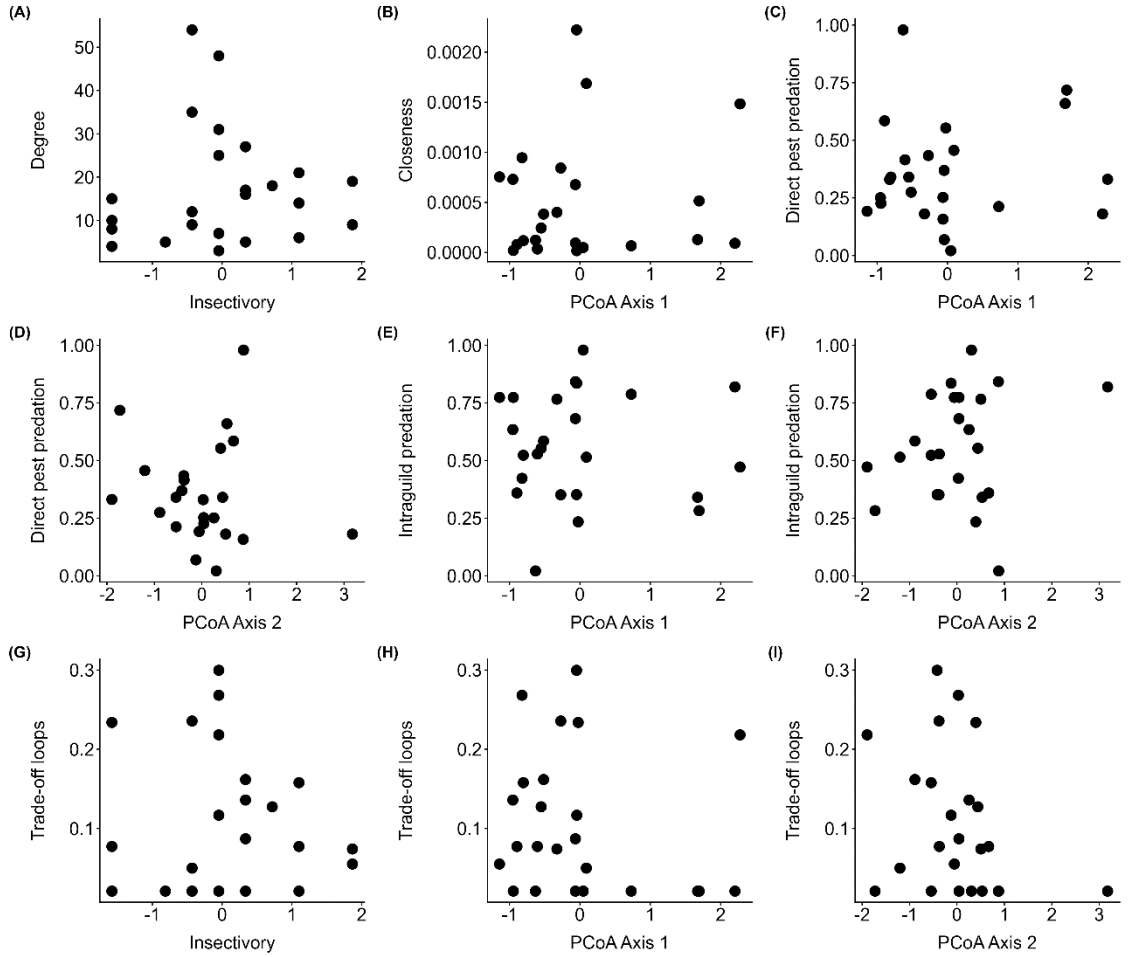

Fig. S1.8. Non-significant relationships between bird insectivory and morphology (PCoA axes), and centrality metrics (A-B) or the proportion of interaction motifs (C-I) in the apple network. Points represent bird species.

Appendix S2
Birds and bats differ in pest control pathways in fruit orchards: intraguild and direct predation

Sensitivity analysis of the apple tri-trophic network using temporally matched samples (June subset)

To address concerns regarding temporal mismatches among datasets, we conducted an additional analysis restricted to bird and bat samples collected in June (54 and 72 samples, respectively), corresponding to the period when spider communities were sampled in apple orchards. In total, we analysed 54 samples from nine bird species from apple orchards, 72 samples from three bat species from roosts nearby the study orchards, and 210 samples from 48 spider species from apple orchards. This subset ensures temporal overlap among trophic levels and allows assessing the robustness of the main network structure and inferred interaction patterns under consistent sampling conditions. The methodological approach followed is identical to that described in the main text. Results from this temporally matched subset were qualitatively consistent with those obtained using the full dataset. Below, we present the corresponding results.

Tritrophic network

The apple tritrophic network from the subset of June samples contained nine bird, three bat, 32 spider species, and 54 pest species, as well as 190 interaction events (Fig. S2.1A). Birds accounted for 43% of the total interactions, bats for 27% and spiders for 31%. As expected, the values obtained in the rarefaction analysis of the bipartite networks were lower than those from the apple tri-trophic network with all samples. Some of these values dropped below 50% of sample coverage (Fig. S2.2).

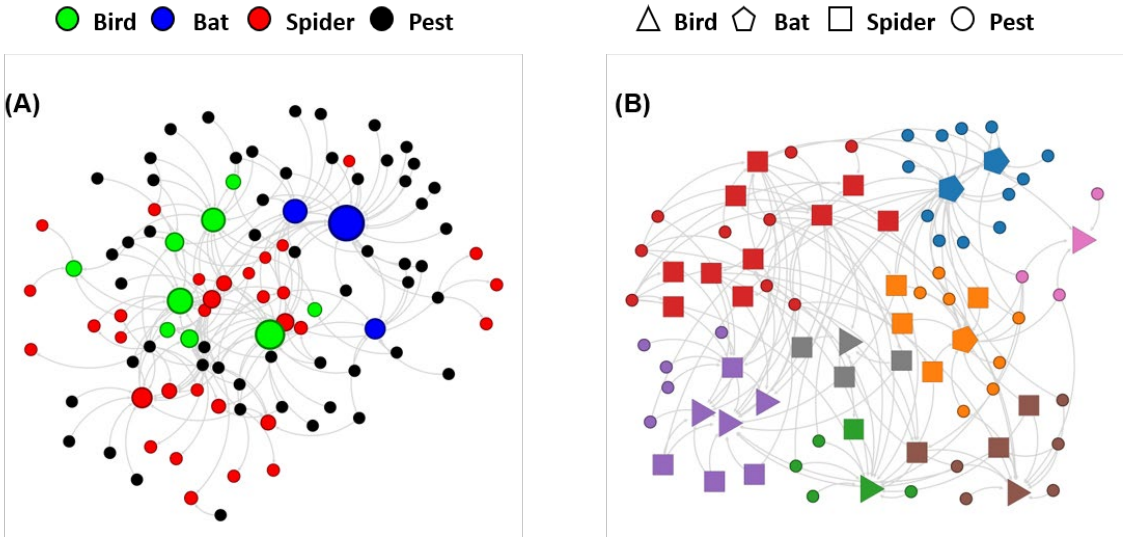

Fig. S2.1. Structure of the apple tritrophic network from the subset of June samples. (A) Nodes represent taxa, with colours indicating the group (i.e., birds, bats, spiders, and pests), links represent interactions. Size of nodes is scaled with taxon's in-degree. (B) Subnetwork containing the eight largest modules (comprising 82% of all taxa). The nodes have been placed ad hoc to emphasize module display. The colours of nodes (taxa) indicate the module, shapes the group (i.e., birds, bats, spiders, and pests).

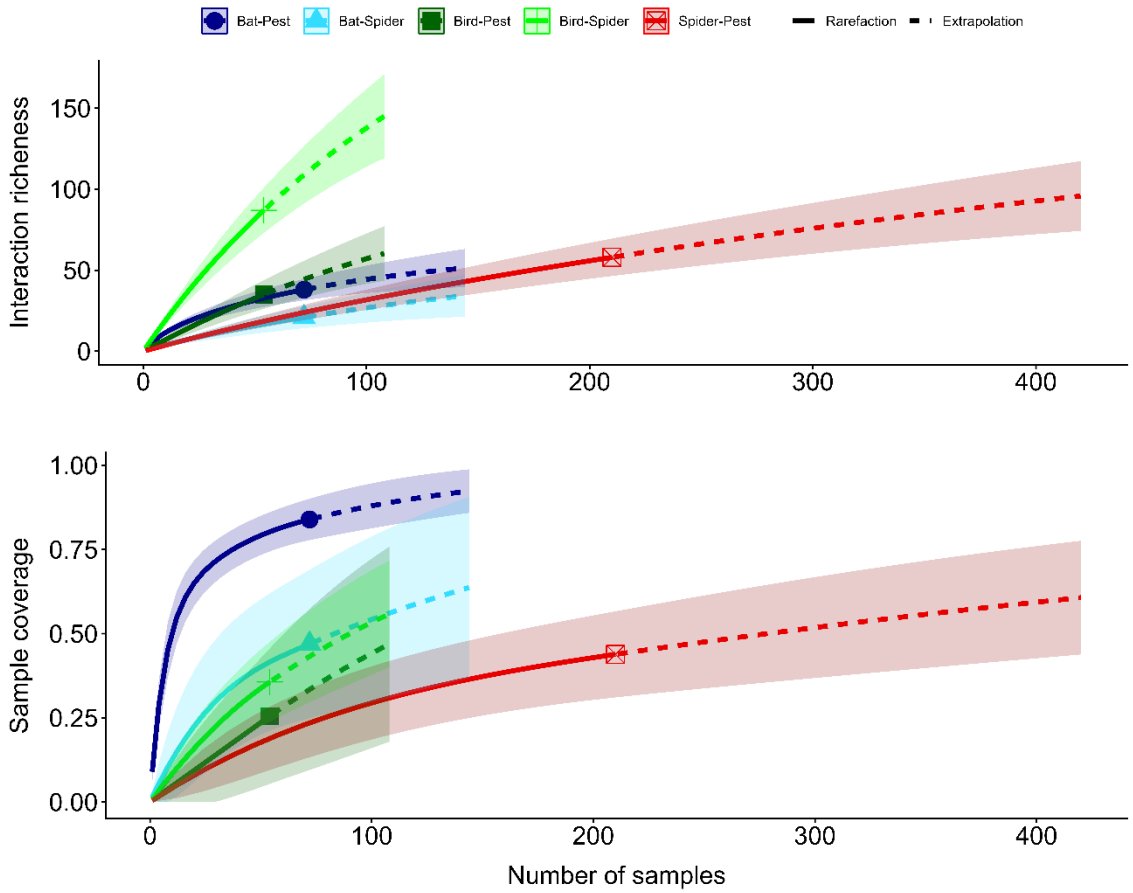

Fig. S2.2. Rarefaction curves of predator-prey interactions richness and sample coverage, per sampling effort unit (number of samples of predatory species analysed), for different interaction types. Symbols represent the observed values and the dashed line the extrapolated values expected with higher sampling effort.

Network modularity

The Infomap algorithm detected 13 modules. This degree of modularity was higher than anticipated by random processes based on species abundances (Fig. S2.3). Eight large modules encompassed 82% of the interacting species (Fig. S2.4). Birds and bats were in different modules. In addition, some modules comprised a single predator group coupled to pests, indicating that distinct consumer types aggregate different sets of pests within modules (Fig. S2.1B).

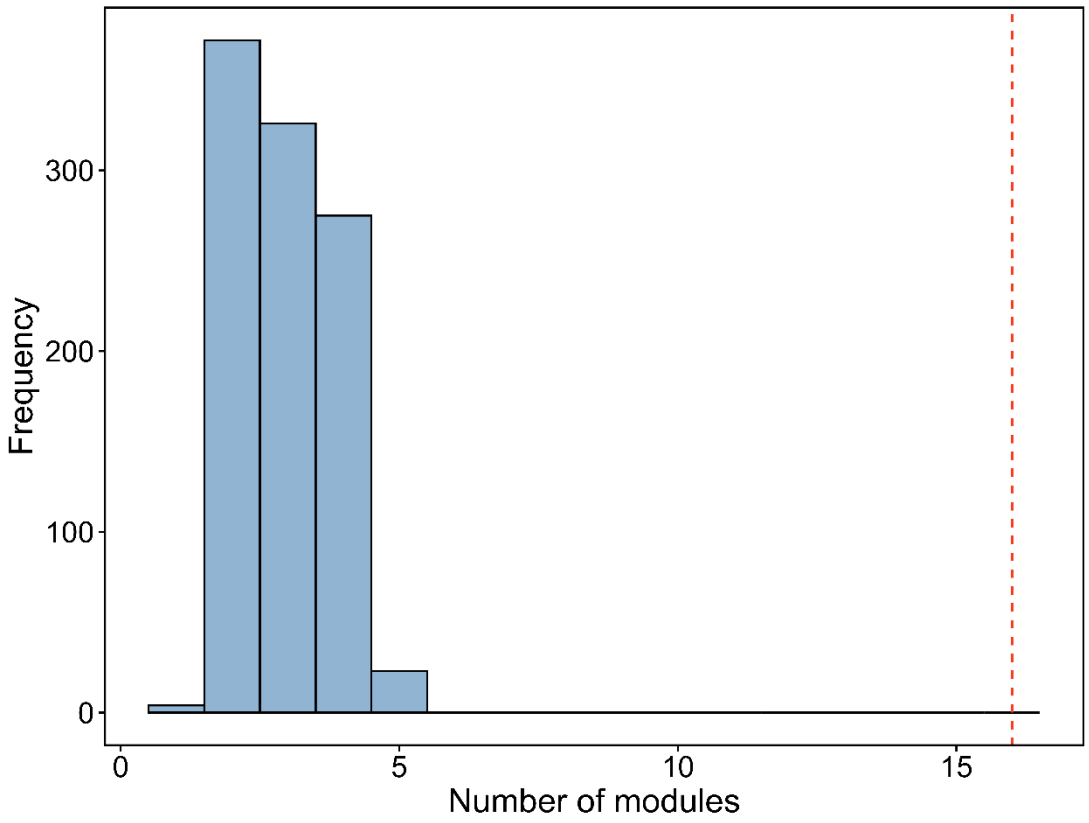

Fig. S2.3. Histogram with the frequency of the number of modules of 1,000 randomized networks originated by the Vaznull null-model. Red dashed line despites the number of modules in the observed tritrophic network.

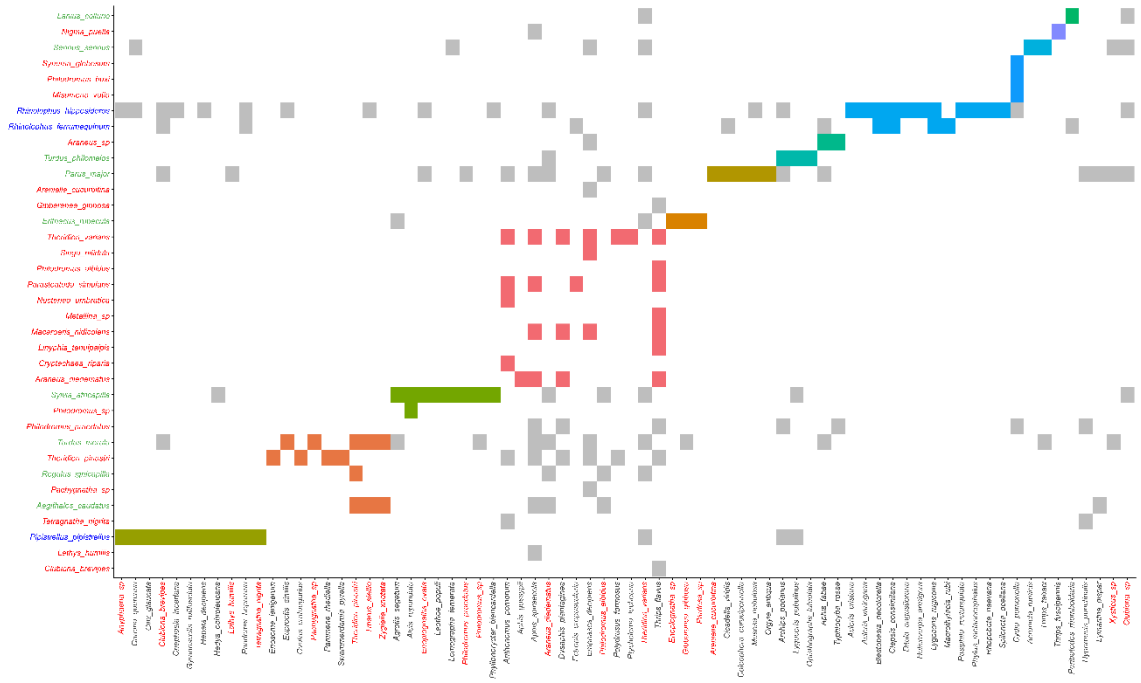

Fig. S2.4. Representation of the apple tritrophic network from the subset of June samples between vertebrates (birds in green and bats in blue), spiders (in red) and pests (in black). Actual interactions between taxon pairs are shown in coloured squares. Each

colour represents interactions between taxon pairs belonging to the same module, and the grey squares represent those between taxon pairs belonging to different modules.

Topological and tri-trophic roles of bird and bat species

Centrality metrics did not reveal differences between birds and bats species within the interaction network (degree: $\beta = -0.64$; $p = 0.08$; harmonic closeness: $\beta = -1.12$; $p = 0.13$; undirect betweenness positive-part: $\beta = 0.00$; $p = 1.00$), likely attributable to the highly variability observed within each group (Fig. S2.5A). As observed in the apple network with all samples, *Pipistrellus pipistrellus* exhibited the highest harmonic closeness and undirected betweenness values, indicating a structurally significant position within the network. However, this was not sufficient to elicit significant differences between the groups.

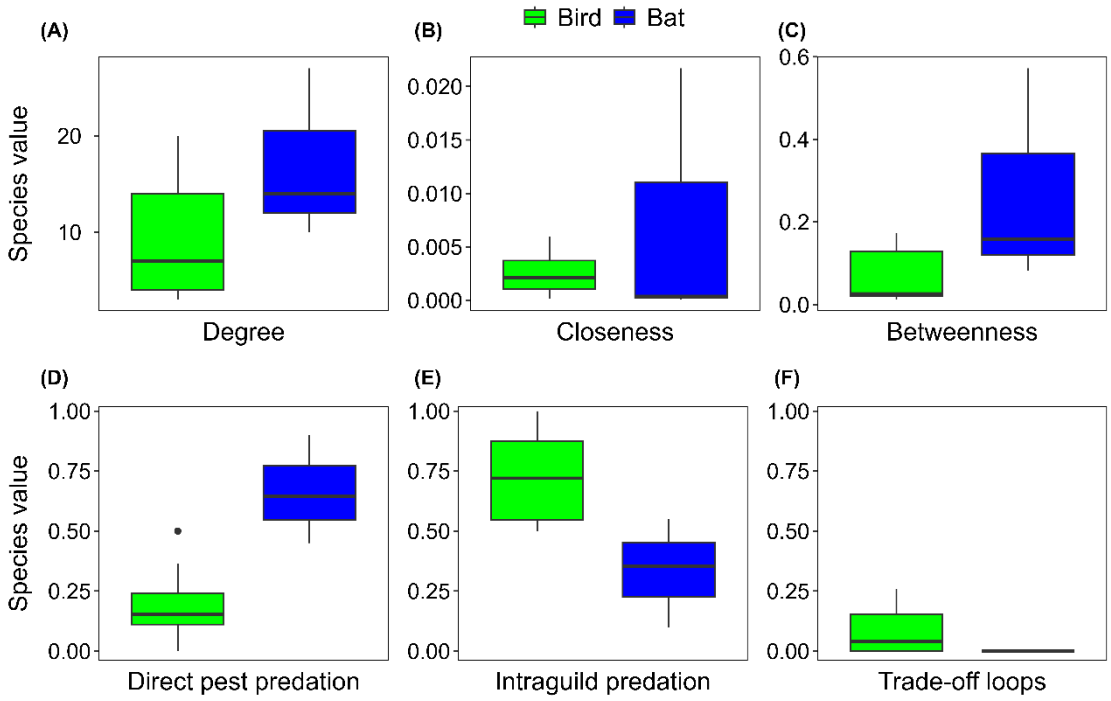

Fig. S2.5. (A-C) Values of centrality metrics for bird and bat taxa within the tri-trophic network. (D-F) Proportion of interaction motifs for bird and bat within the tri-trophic network.

In total, we detected 205 motifs involving trophic cascades from top predators to pests. 61% corresponded to intraguild predation, 31% to direct pest predation and 8% to trade-off loops. The distribution of motifs was not equal between birds and bats (Fig. S2.5B). Bats showed a higher proportion of direct pest predation, involving 62% of motifs, than birds, a difference supported by the beta regression ($\beta = -1.88$, $p < 0.01$). Meanwhile, intraguild predation was the most frequent motif in birds, accounting on average for 70% of motifs. We also found difference between groups for intraguild predation ($\beta = 1.50$, $p < 0.01$), but not for the trade-off loops ($\beta = 0.63$, $p = 0.21$). The position of top predators in the network was a poor indicator of the type of trophic cascades in which they were involved. We only found a positive correlation between the proportion of trade-off loops with the degree ($\beta = 0.67$, $p = 0.02$).